Direct evidence of CO_2 drawdown through enhanced weathering in soils

Tobias Linke (tol5@hi.is)
University of Iceland, Institute of Earth Sciences
Eric H. Oelkers
University of Iceland, Institute of Earth Sciences
Susanne C. Möckel
University of Iceland, Institute of Life and Environmental Sciences
Sigurdur R. Gislason
University of Iceland, Institute of Earth Sciences

Research Article

Keywords: Enhanced Rock Weathering, Alkalinity export, Andosol

Posted Date: October 16th, 2023

DOI: https://doi.org/10.21203/rs.3.rs-3439312/v1

Abstract

The ability of engineered enhanced rock weathering to impact atmospheric CO_2 has been challenging to demonstrate due to the many processes occurring in soils and the short time span of current projects. Here we report the carbon balance in an Icelandic Histic/Gleyic Andosol that has received large quantities of basaltic dust over 3,300 years, providing opportunity to quantify the rates and long-term consequences of enhanced rock weathering. The added basaltic dust has dissolved continuously since its deposition. The alkalinity of the soil waters is more than 10-times higher than in equivalent basalt-dust-free soils. After accounting for oxidation and degassing when the soil waters are exposed to the atmosphere, the annual CO_2 drawdown due to alkalinity generation is 0.17 tC ha^{-1} yr^{-1}. This study validates the ability of fine grained mafic mineral addition to soils to attenuate increasing atmospheric CO_2 by alkalinity export. Induced changes in soil organic carbon storage, however, likely dominate the net CO_2 drawdown of enhanced weathering efforts.

Introduction

The natural weathering of basaltic and ultramafic rocks has been demonstrated to have a relatively large role in the drawdown of CO_2 from the atmosphere [1–4]. Such observations have motivated several research groups to propose using these rocks to remove CO_2 directly from the atmosphere through a process called Enhanced Weathering (EW) in an attempt to limit future global warming [5–7]. Enhanced weathering involves amending soils with crushed fine-grained, fast-reacting Ca-Mg-silicate rocks and minerals such as basalts and peridotites [8]. To date, enhanced weathering field experiments have demonstrated improved crop vigor, organic and inorganic carbon storage and decreased N_2O degassing [7,9,10]. One of the goals of this enhanced weathering approach is to increase the alkalinity export of waters that drain from soils and enter rivers and streams. Enhanced weathering field studies to date have yet to identify or quantify alkalinity export enhancement due to several factors including the large number of processes that occur in soils, and the short duration of these field studies.

One approach to investigating the long-term behavior and consequences of anthropogenically influenced terrestrial processes such as enhanced weathering is via natural analogues. Enhanced weathering experiments to date have tested the addition of up to 400 t ha^{-1} yr^{-1} of crushed Ca-Mg-silicate rocks to agricultural soils [11–15]. This crushed rock flux is orders of magnitude higher than estimates of global desert dust deposition on Earth, which is estimated to average up to 0.5 t ha^{-1} yr^{-1} [16]. In the vicinity of the dust “hot spots” on Earth, such as South Iceland, however, the mass of deposited fine grained basaltic dust can be as high as 8 t ha^{-1} yr^{-1} [17–19]. Although the natural mass flux of basalt added to South Iceland Histic/Gleyic Andosols is less than that of current EW efforts, 1) this flux of basalt dust has been added continuously to the soil of this region over at least the past 3,300 years, such that in total over 16,500 t ha^{-1} of basaltic dust has been added to this soil over this time, and 2) the specific surface area of natural basaltic dust is likely substantially higher than that added to the soils in current EW

experiments due to its finer grain size. The grain size of the crushed rocks used in EW-applications, if reported, is commonly less than 150 μm [9,13]. In contrast, the average size of basaltic Icelandic dust ranges from 10 to 62 μm [19–21]. For these reasons, South Icelandic vegetated Histic/Gleyic Andosols provide an insightful natural analogue to illuminate the long-term effect of EW-applications performed under similar climate, vegetation, and soil conditions.

This study is focused on a natural analogue to quantify the long-term consequences of the addition of ground basalt on the carbon balance in soils. The natural analogue considered in this study is a mineral rich Histic/Gleyic Andosol in South Iceland [22,23]. It receives large amounts of air-borne volcanic material during 1) explosive volcanic eruptions in the form of glassy volcanic ash fallout referred to as tephra, and 2) dust storms caused by the transport of fresh and or partly weathered volcanic ash [18,24]. These events lead to evident tephra horizons that can be used to date these soils. The annual dust fallout is finer grained than the tephra and intermingled with the soil organic carbon. Based on paleoecologic research [22,25–27], in the absence of this volcanic dust input, the Histic/Gleyic Andosols of Southern Iceland would have developed into Histosols [28]. Consequently, the comparison of the chemical behavior of South Icelandic Histic/Gleyic Andosols with that of volcanic dust-free Histosols, located in similar climatic zones provides insight into the long-term consequences of adding fine grained basaltic material to soils as part of enhanced weathering efforts.

The motivation to focus on the addition of volcanic material to Histosols/peat soils to drawdown CO_2 from the atmosphere stems from the substantial role of these soils in the global carbon cycle. Peatlands connect the Earth's terrestrial and aquatic ecosystems. Although they cover only about 3% of the continents [29], they store ~ 10% of all non-glacial freshwater and 300 to 450 GtC, or roughly 30% of the land-based organic carbon [30–32]. Man-made drainage and burning of peat areas world-wide releases 0.5–0.8 GtC yr^{-1}, which is equivalent to 5–8% of global anthropogenic carbon emissions [33–35]. Carbon dioxide emission from the drainage of peat areas is estimated to be the largest anthropogenic source of CO_2 emission in Iceland [36].

The detailed study of a South Iceland field site, experiencing annual natural basaltic dust inputs, is used in this study to quantify its ability to generate alkalinity. A comparison of the alkalinity export from this soil with corresponding results from volcanic dust-free Histosols is used to quantify directly the ability of enhanced rock weathering efforts to drawdown CO_2 from the atmosphere. Results are then used to estimate the potential efficiency of enhanced weathering at a larger scale. The purpose of this paper is to present the results of this study and use the results to gain insight into the long-term consequences of current and future enhanced weathering efforts.

Field site description

The field site chosen for this study is located above the source of the Rauðalækur ("Red creek") river at 63°53'42.5"N 20°21'15.9"W. This site is approximately 7 km north of the town of Hella in South Iceland.

The soils in the area are dominated by Brown and Gleyic Andosols, although some Histic Andosols are common locally [22,37]. Our study site consists of an upper Gleyic Andosol and a lower Histic Andosol (see the on-line supplement for further details). The study site receives an annual aeolian dust flux of 5–8 t ha^{-1} yr^{-1}, consisting of mostly basaltic glass [18]. Additional quantities of basaltic material are added during irregular volcanic events. During the past several decades, drainage trenches have been cut into the nearby soils; the closest drainage ditch is located more than 150 meters from the study site. The studied soil contains several prominent horizontal tephra layers, of basaltic to rhyolitic composition with thicknesses ranging from a few mm to few cm and deposited during the past 3,300 years. The tephra layers correspond to specific volcanic eruptions, allowing the direct dating of the rate of soil accumulation over time. An image and schematic illustration of the system is provided in Fig. 1 and a detailed description of the field site, and the soil section are provided in the online methods and Supplementary Information Table SI1.

Results

Fluid Compositions

Soil fluid samples were collected using suction cup samplers from May to November 2018. The compositions of all collected fluid samples are provided in Table SI2 and the measured compositions of fluids for selected elements are shown as a function of depth in Figure 2. The pH of the samples were recalculated using PHREEQC [38] to the in-situ soil temperature of 7 °C. This is the average soil temperature at 76-260 cm depth during the summer months [39]. The concentrations of major elements increase continuously with depth suggesting the continuous dissolution of the basaltic dust over the whole extent of the soil. The soil waters become increasingly anoxic with depth as indicated by the Eh values shown in Figure 2b.

The alkalinity of the soil waters increases from 0 to 3 meq kg^{-1} with depth. Dissolved organic carbon in the soil water samples is about 10 % of dissolved inorganic carbon. Once these waters exit the soils, they will equilibrate with the O_2 and CO_2 in the atmosphere. PHREEQC calculations indicate that the alkalinity of the soil waters will decrease on average to 1.53±0.2 meq kg^{-1} due to iron oxidation/precipitation reactions when they come in contact with the atmosphere as they flow into local rivers.

The alkalinity of soil waters in the studied Icelandic basaltic dust-rich soil are compared to corresponding measured alkalinities of basalt-dust-free Histosols located in non-carbonate terrains as a function of pH in Figure 3. Our Icelandic field site, mostly fed by rainwater, shows considerably higher alkalinity and pH values than observed in corresponding basalt-dust-free Histosols. Note that Histosols located in carbonate terrains are not included in this comparison as the presence of carbonate minerals leads to a pH and alkalinity increase due to the dissolution of the carbonates, a process which has no net long-term effect on atmospheric carbon drawdown. The comparison in Figure 3 shows clearly that the addition of volcanic dust to the soil of our study site has increased substantially the alkalinity in its soil waters, most

notably deep in the soil column. This observation confirms the ability of enhanced weathering by the addition of basaltic dust to soils to draw down CO_2 from the atmosphere.

Measured alkalinity of soil waters, collected from systems having little to no interaction with bedrock, as a function of pH. The black symbols correspond to alkalinity values reported in the literature for Histosols from bogs, poor or rich fens located in non-volcanic regions and in the absence of carbonate bedrock, whereas the red, orange, green and blue symbols represent soil water samples measured in the present study at the depths indicated in the figure. The purple symbol shows the composition of rainwater at our field site. The sources of the literature data shown in this figure and their sampling locations and further details are provided in Table SI3.

A noteworthy observation is that the basaltic dust in the studied soil column persists and is reactive throughout the soil column, despite the fact that some of this dust has been present in the soil for 3,300 years. This observation is consistent with mass balance estimates of the import and export of metals to the soil column. The study site receives an average annual dust flux of 500-800 g m^{-2} yr^{-1}. This mass of basalt would add 0.96-1.54 mol Ca and 0.72-1.16 mol Mg per m^2 yr^{-1} to the soil. In contrast, the average Ca and Mg concentration of the deep soil water is 5 x 10^{-4} and 4 x 10^{-4} mol kg^{-1} for Ca and Mg, respectively. Taking account of the estimated 925±150 kg m^{-2} yr^{-1} of water that flows through and is exported annually by our studied soil (see online methods for details of this water-flow estimate), we estimate that 0.47±0.07 and 0.37±0.06 mol yr^{-1} of Ca and Mg are removed from the soil per square meter of soil surface area at the present time. The input of Ca and Mg by volcanic dust addition is, therefore, approximately 2-3 times more than that removed by soil water export. The results of this comparison are consistent with the persistence of the reactive dust throughout the soil column and suggest the long-term viability of enhanced weathering efforts.

Carbon Storage via alkalinity export by the addition of basaltic material to soils

The rate of carbon drawdown due to alkalinity export by enhanced weathering in our studied field site can be estimated by combining the annual water flux through the soil and the measured alkalinity. By taking account of the rainfall, evaporation, and surface runoff it is estimated that 925±150 kg m^{-2} yr^{-1} of water pass through and are exported from the studied soil annually. Multiplying this number by the 1.53±0.2 meq kg^{-1} average alkalinity of the deepest water samples of our study area, after its equilibration with the atmosphere, yields an estimated alkalinity export from our soils of 1.43±0.3 eq m^{-2} yr^{-1}. Multiplying this number by the atomic weight of carbon yields an annual carbon addition to our river water of 17±3.6 g m^{-2} yr^{-1}, which equals 0.17±3.6 t ha^{-1} yr^{-1} of C.

It is insightful to extrapolate this annual rate of carbon drawdown to a larger scale. If the results of our studied field site are representative, the removal of 1 Gt yr^{-1} CO_2 from the atmosphere through alkalinity production would require a total of 16 million km^2 of surface. This is larger than the total surface area of the United States. Moreover, the mass of basaltic dust required to provoke this rate of carbon removal

may be unrealistically large. The average annual flux of basaltic dust into the studied South Iceland soils is 5-8 t ha^{-1} yr^{-1}. Adding this mass of basalt over 16 million km^2 of surface would require 8 to 13 Gt of finely ground basalt annually. This mass of ground basalt is larger than the world's annual cement production of 4.3 Gt in 2020 (iea.org/reports/cement). It should be noted, however, that the alkalinity generated in our studied Histic/Gleyic Andosol was the consequence of the dissolution of the basalt added to this soil annually over the past 3,300 years. This annual addition has led to a buildup of basaltic material over time. The results shown in Figure 2 indicate that the presence of older basaltic dust, located deep in the soil profile is an important contributor to alkalinity production. As such, it seems likely that substantially more than 5-8 t ha^{-1} yr^{-1} would need to be added to soils near-term as part of enhanced weathering efforts to provoke a similar rate of alkalinity production as observed in our study area.

One additional caveat to applying alkalinity generation from enhanced weathering of soils on the continents to global carbon drawdown from the atmosphere is the fate of soil generated alkalinity after its transport in rivers to the oceans. The exact mass of CO_2 removed from the oceans due to alkalinity input is currently debated, but is likely attenuated by carbonate mineral precipitation [39–41]. Recent estimates suggest a CO_2 uptake efficiency of only 0.6 to 0.8 mol of CO_2 for each mole of alkalinity added to the oceans [42]. Such observations suggest that the total carbon drawdown from the atmosphere by alkalinity generation on the continents will depend on the eventual fate of this alkalinity and it is likely decreased by marine processes.

Carbon drawdown by alkalinity production versus soil organic carbon

A substantial mass of carbon is stored by soils in organic material. The rate of organic carbon buildup in our studied soil can be estimated by taking account the rate of soil formation and the organic content of this soil. The average soil formation rate at our study site is estimated to be 0.067 cm yr^{-1}. This estimate is made by dividing the current 2.2 m soil thickness by 3,300 years, the time the soil developed (see Fig. 1). The organic carbon content of the studied Histic/Gleyic Andosol is between ~12 % and 20 % of the dry mass and it has a porosity between 50 % and 75 % [43,44] as described in the online methods section. The combination of this range of carbon content and porosity values yield an estimated total mass of organic carbon stored in this soil equal to 86-172 kg C m^{-2}. The total mass of carbon estimated in our study area compares well with corresponding estimates of Óskarsson et al. (2004) [45], who estimate the C stocks of Histosols in Iceland to be on average 197 kg C m^{-2}, and the more mineral-rich Histic Andosols in Iceland to be 89 kg C m^{-2}.

The average net annual rate of carbon drawdown in our soil due to organic carbon buildup can be estimated by dividing the 86-172 kg C m^{-2} of organic carbon present in the soil by the 3,300 years of soil development. This calculation yields an estimated 26-52 g C m^{-2} yr^{-1} drawdown due to net organic carbon production. This estimated value of carbon drawdown is substantially larger than the 17±3.6 g C m^{-2} yr^{-1} drawdown of CO_2 due to alkalinity export in our studied soils. These estimates, that are in agreement with previous studies [4], also suggest that the amount of CO_2 removed by the addition of basaltic dust to the

soil in one year by alkalinity export is more than 3 orders of magnitude less than the total CO_2 stored as organic carbon in the soil. This latter observation should serve as a warning to those attempting atmospheric CO_2 drawdown by enhanced weathering in soils. If the addition of basaltic dust to soil leads to the accelerated decomposition of organic material in soils, the latter process could readily dominate leading to a net increase of CO_2 released to the atmosphere due to enhanced weathering efforts.

The degree to which the addition of basalt increases or decreases the total mass of organic carbon in a soil is currently poorly constrained. Vicca et al. (2022) [46] argued that the efficiency of enhanced weathering effort is governed by biologic processes. These authors noted that nutrients released by the addition of ground rocks to soils could enhance plant growth and promote organic carbon storage in soils. They also postulated that the addition of this material could accelerate organic material decay in the subsurface. Goll et al. (2021) [47] suggested that the addition of basalt to soils would improve the fertility potentially, enhancing organic carbon storage in soils. Some supporting evidence was reported by Angst et al. (2018) [48], who observed that soils derived from a basaltic rock stored more organic carbon than soils derived from sandstone or from loess. This was interpreted by these authors to be due to a combination of a higher clay content and greater availability of nutrients in the basalt derived soils. Similarly, da Silva et al. (2016) [49]concluded that the organic carbon content of soils derived from granitic rocks increased with increasing mafic content of the parent rock due to increased clay mineral content. Möckel et al., (2021a, 2021b) [50,51] provided evidence that volcanic mineral dust, and soil and tephra layers hamper organic carbon decomposition in Histosols of natural peatlands in Iceland. In contrast, other studies found that soil parent material and mineral oxide compositions have little effect on the mass of organic carbon in soils [52]. One factor that is clearly detrimental to the preservation of soil organic carbon is tilling. Soil tilling has been shown to accelerate greatly soil organic carbon degradation [53–55]. Such observations suggest that the way that basaltic dust is added to soil during enhanced weathering efforts may be critical for increasing the net carbon drawdown in these soils. In either case, consideration of the relative rates of carbon drawdown through inorganic compared to organic processes presented in this study suggests that the latter may dominate the net carbon storage in soils due to enhanced weathering. This makes the quantification of the role of basaltic dust on productivity and organic preservation a critical factor in optimizing enhanced weathering efforts.

Schematic illustration of the processes drawing down CO_2 at our studied Southern Icelandic field site. The site receives ~1250±200 kg m^{-2} yr^{-1} of rainfall. Of this rainfall 16 % is estimated to evaporate and 10 % is estimated to be lost to surface runoff. While the remaining 925±150 kg m^{-2} yr^{-1} of water passes through the soil, its alkalinity increases on average from 0 to 2.59±0.34 meq kg^{-1} at depth. Once these waters equilibrate with the atmosphere, this fluid oxidizes and some CO_2 is released such that the alkalinity decreases to 1.53±0.2 meq kg^{-1} resulting in an annual export of 17±3.6 g C per m^2 soil surface area. At the same time 26-52 g m^{-2} yr^{-1} of C is drawn down from the atmosphere by organic carbon production and stored in the soil.

Conclusions

The results of this study confirm the ability of the addition of fine-grained basaltic rock to soils to enhance CO_2 drawdown directly from the atmosphere due to alkalinity production. In total it is estimated that 17 ± 3.6 g C m^{-2} yr^{-1} is currently drawn down and added to rivers by alkalinity production from our South Iceland field site. The enhanced alkalinity production of our soils was produced by the addition of approximately 1.7–2.6 t m^{-2} of basaltic dust to this soil over 3,300 years. Upscaling of this process to address even a small fraction of the mass of anthropogenic CO_2 emissions to the atmosphere, however, may be challenging for two reasons: 1) this enhanced weathering process is slow and would require more land than what is available for a sizeable drawdown of anthropogenic CO_2 through alkalinity production and 2) the here to date unquantified effect of adding basalt powder to soils on soil organic matter. So, although this study serves as a proof of concept of the potential of enhanced weathering efforts to contribute to attenuating atmospheric CO_2 concentrations, the degree to which this approach will prove successful at a larger scale remains unclear.

Online Methods

Soil classification and soil evolution in Iceland

Iceland is built of volcanic rocks, which are predominantly (80–85%) of basaltic composition, the remainder being intermediate and silicic volcanics and clastic sediments that are mostly of basaltic composition [56]. The oldest exposed rocks are about 15 Myr [57]. Iceland was fully covered with glaciers at the Last Glacial Maximum (~ 20 kyr BP). The ice sheet retreated close to the present coastline around 10.3 kyr BP, and at about 8.0 kyr BP Icelandic glaciers were of similar, or little lesser extent, than at the present [58]. Hence, all Icelandic soils are of Holocene age younger than ~ 10 kyr BP [28].

Andosols are the dominant soils in Iceland, Vitrisols are present in desert areas and organic-rich Histosols are found in some wetland areas [28]. Andosols are not common in Europe, but they are widespread in the active volcanic areas of the world [28]. Two main factors are commonly used to classify Icelandic soils: deposition of aeolian (volcanic) material and drainage [23]. Aeolian material mostly originates from the sandy desert areas located near active volcanic zones or from glaciofluvial outwash plains. After the settlement in Iceland, around 1076 year BP, the extent of barren areas that are a source for aeolian material significantly increased [27,59]. Andosols are often found in the wetland areas of Iceland where substantial aeolian input is present, lowering the relative organic content, or where some drainage is present. Whereas organic-rich Histosols are found in wetlands with little aeolian input. The progression of soil types with improving drainage conditions from wet to dry follows: Histosols (> 20% C), Histic Andosols (12–20% C), Gleyic Andosols (< 12% C, poorly drained), and Brown Andosols (< 12% C, freely drained) [28]. This order also reflects the decreasing distance from the volcanic zones and the source of aeolian materials. The transition between these soil types is fluent, and changes in drainage or aeolian input can lead to a change of the soil type. It is postulated that in absence of the volcanic influences,

Icelandic wetland soils would largely be organic Histosols, typical of the arctic environments [22,28]. This suggests that applying EW and the addition of basaltic dust to an organic-rich Histosol can lead to its transition to a more mineral-rich soil such as an Andosol, as found in our study area.

Histosols or peatlands are classified further as *ombrotrophic* or *minerotrophic*, based on the origin and mineral content of the waters feeding them [60]. While *minerotrophic* soils receive mostly ground water that has interacted with the bedrock upstream leading to an enrichment of the mineral content in the water, *ombrotrophic* soils are dominantly fed by rainwater, and are therefore nearly free of rock derived dissolved constituents [60]. Our studied field site receives mostly rainwater. Therefore, all dissolved constituents in our soil water are assumed to originate from the interaction of rainwater with the embedded dust of our soil, and the decay of organic matter. Based on this assumption, we compare our data (see Fig. 3) with data from other sites reported in the literature as mostly *ombrotrophic*, implying limited interaction with the underlying bedrocks.

Detailed field site description

The field site is located above the source of the Rauðalækur (“Red creek”) river at 63°53'42.5"N 20°21'15.9"W, 7 km north of the town of Hella, South Iceland. This field site has not been used for agriculture or fertilized for at least the past 10 years prior to this study, limited anthropogenic contamination is therefore expected. Based on data from the Icelandic Meteorological Office, the average soil temperature is ~ 7°C during the summer [61]. At 100 cm soil depth, the annual maximum temperature is 9°C and the annual minimum temperature is 1°C. The soil can, however, temporarily freeze down to a depth of 50 cm [61]. The annual rainfall in this area is 1250 ± 200 mm. The average storm yields an average of 15 mm of rain with a maximum duration of 20 hours (www.en.vedur.is/climatology/data). The surface of the studied soil is hummocky, and the vegetation is characterized by graminoids with a clear predominance of Poaceae. The direction of the groundwater flow, estimated based on the surrounding drainage channels, is towards S/SE. Based on field observations, the groundwater table fluctuates near a depth of 50 cm.

The field site is adjacent to a natural escarpment allowing for the characterization of the subsurface soil profile. Several tephra layers were identified within a cleared vertical face of the escarpment. Layers of organic-rich soil admixed with air-borne basaltic dust separate the tephra layers. The dust in these layers is finer grained than the basalt in the tephra layers. The tephra layers can be assigned to specific volcanic eruptions, as each volcanic eruption in Iceland has its own chemical fingerprint [59,62]. These allow determination of the soil accumulation rates. As can be seen in Fig. 2b, over the last 3,300 years about 220 cm of soil has accumulated, averaging to a soil thickening rate of 0.067 cm yr^{-1}. The ‘Settlement layer’, a tephra layer from an eruption of the Vatnaöldur volcanic system at 1079 ± 2 BP [62], which approximately coincides with the initial settlement (Landnám) of Iceland, was barely discernible in the soil profile. Although the exact depth of this Settlement tephra at around 96 cm depth is somewhat uncertain, its location suggests an average soil accumulation rate of 0.086 cm yr^{-1} during the last 1120

years. This is consistent with Gísladóttir et al. (2011) who reported that the dust flux over South-Central Iceland increased following the emplacement of the Settlement layer [63]. A detailed description of the soil profile is provided in Table SI1 of the Supplementary Information following the guidelines provided in Schoeneberger et al. (2012) [64].

Details of field sampling

In-situ soil waters were sampled 10 m North from the escarpment in the field with suction cup samplers obtained from Prenart, Denmark. Four suction cup samplers were installed into holes drilled at an angle of 60° at depths of 76, 121, 173, 260 cm on November 8th, 2017, following the method of Sigfusson et al. (2006) [65]. The samplers were left in the field over the winter to allow settling of the soil around the samplers and tubing. The first samples from these suction cup samplers were collected during May 2018 and the last were collected 21 November 2018. The suction cup samplers, which are 95 mm long and 21 mm in outer diameter, consist of a 48/52% mixture of Polytetrafluorethylene (PTFE) and quartz with an average pore size of 2 µm. These samplers were connected by 1.8 mm inner diameter Teflon (Fluorinated ethylene propylene) tubing to the surface. Sixty ml syringes located at the surface were connected via 3-way valves and 100 cm long connection polyethylene tubing to the Teflon tubing of the subsurface samplers. The first 30–50 ml of extracted soil water during any sampling was discarded to avoid contamination. It took about 6–8 hours to fill the 60 ml sampling syringes. During the sampling the syringes were kept in a closed cooling box to prevent heating and exposure to sunlight. This approach was adapted to avoid any degassing of the soil solutions and oxidation of the samples. No color change of the soil solutions due to iron oxidation was observed during the sampling.

Initial sample analysis was performed in the field including sample pH, temperature and Eh measurements, conductivity determination and H_2S titration. Subsamples for major and trace element analysis via ICP-OES and ICP-MS as well as for ion chromatography to determine Fe^{2+}/Fe^{3+}, DOC analysis and alkalinity titration were collected and stabilized on site and analyzed later in the lab.

Analytical Methods

The redox potentials (E_{meas}) of the collected fluids were measured directly in the sample syringes in the field using a Microelectrodes Inc MI-800 Micro-ORP Ag/AgCl micro combination redox electrode with a ± 10 mV uncertainty. These values were converted to equivalent potentials for a standard hydrogen electrode (E_{SHE}) using a + 199 mV reference potential, E°, for the Ag/AgCl electrode [66]. This calculation was performed using the Nernst equation,

$$E_{SHE} = E_{meas} + \ln(10) \cdot (R \cdot T)/F \cdot pH + E^{\circ}_{Ag/AgCl}$$

where R refers to the gas constant, F designates the Faraday's constant, and T symbolizes the temperature T in kelvin. Subsequently, ~ 5 ml of each sampled fluid was transferred into 10 ml

polypropylene vials for pH temperature, dissolved oxygen, and conductivity measurement. The pH was measured using a Eutech pH 6 + electrode with an uncertainty of ± 0.01 pH units. The dissolved oxygen and conductivity of the samples were measured using a Micro electrodes MI-730 Micro-Oxygen Electrode with an uncertainty of ± 0.5% and a Eutech COND 6 + with an uncertainty of ± 10 µS, respectively. For major and trace element analysis, 10 ml of each fluid sample was first filtered through 0.2 µm cellulose acetate in-line filters then transferred into acid washed polypropylene bottles. A small quantity of 65% Merck suprapure HNO_3 was added to acidify these samples to 0.5% HNO_3. Samples for iron speciation measurement were first filtered through 0.2 µm cellulose acetate in-line filters then placed into acid cleaned polypropylene bottles. Merck HCl was added to these samples to attain a final acid concentration of 0.5%. Samples for dissolved organic carbon analysis were collected in acid washed polycarbonate bottles and acidified with 0.5 M suprapure, Merck HCl to a final acid concentration of 3.3%.

Dissolved hydrogen sulfide, H_2S, was determined in the field by precipitation titration immediately after sampling with an uncertainty of ± 0.7 µmol kg^{-1}, using mercury acetate solution $Hg(CH_3COO)_2$ of a known concentration as described by Arnórsson (2000) [67]. Alkalinity titrations were performed immediately after returning the samples to the laboratory. For each titration, ~ 5 ml of fluid was transferred in a 10 ml vial and titrated to pH 3.3 by addition of 0.1 M HCl while constantly stirring the fluid. The pH of the fluid was recorded using a glass pH electrode together with a pH 110, Eutech instruments millivolt meter. The alkalinity was calculated by the Gran method using the inflection points [68]. The final measured alkalinity values are given in meq kg^{-1} with an uncertainty of ±5% or less.

Elemental Analysis

Major element compositions of all fluid samples were determined using a Ciros Vision, Spectro Inductively Coupled Plasma Optical Emission Spectrometer (ICP-OES). The instrument was calibrated using the SEL-11 in-house standard, which was referenced to the SPEX CertiPrep commercial standard material. All standards and measured samples were acidified to 0.5% using suprapure HNO_3 prior to analysis. All measurements were run in duplicate. Blank solutions were measured after every 5 samples and uncertainties were below ±5% for each element.

Iron species were determined using a Dionex 3000 ion chromatography system equipped with a Variable Wavelength Detector using the method described by Kaasalainen et al. (2016) [69]. This method separates Fe^{2+} and Fe^{3+} using pyridine-2,6-dicarboxylic acid (PDCA) as a chelating agent. It detects the distinct Fe cations by post-column derivatization using 4-(2-pyridylazo)resorcinol with a peak absorbance at 530 nm, a detection limit of ~ 2 µg l^{-1} and an uncertainty of ±2% or less for Fe^{2+} and ±10% for Fe^{3+} for 200–1000 µl samples.

Dissolved organic carbon concentrations were determined by size exclusion chromatography using a Liquid Chromatography – Organic Carbon Detection system (LC-OCD) obtained from DOC Labor in Karlsruhe, Germany, following the method of Huber et al. (2011) [70]. The system was calibrated for the

molecular masses of humic and fulvic acids using standard material from the Suwannee River, provided by the International Humic Substances Society (IHSS). All DOC measurements have an uncertainty of 5% or less.

Calculation of alkalinity creation and export in our studied soil

Alkalinity export in our field site was determined by multiplying the mass of water passing through the soil by the alkalinity generated in the soil, taking account the loss of alkalinity as the soil solution interacted with the atmosphere. Any effect of eventual changes in this alkalinity after the fluids arrive in the oceans is not taken into account. The alkalinity of the soil solution after its equilibration with the atmosphere was calculated using the PHREEQC software version 3.4.0 [38]together with the minteq.v4 thermodynamic database [71,72]. This alkalinity was determined from the average of all measured major element concentrations, pH and alkalinity in the deepest soil water samplers (see Tab. ES2). This fluid was equilibrated with atmospheric O_2 concentration. Ferrihydrite is allowed to precipitate at local equilibrium as the fluid oxidized. The resulting fluid was then equilibrated with the 400 ppm CO_2 concentration of the atmosphere to account for fluid degassing.

The mass of fluid passing through the soil was estimated to be equal to the difference between the mean precipitation for the field site minus the evapotranspiration and the direct runoff. The mean precipitation is equal to 1250 ± 200 mm yr^{-1}, based on the records from the measurement station in Hella located ~ 7 km away from the field site operated by the Icelandic Metrological Office Veðurstofa Íslands (https://en.vedur.is/climatology/data). The evapotranspiration at the field site was estimated based on Jóhannesson et al. (2007) [73] to be equal to 16% of the precipitation corresponding to 200 mm yr^{-1}. The direct surface runoff is estimated to be 10%, based on data published by Sigurðsson et al. (2004) [74]. After subtracting the evapotranspiration and direct surface runoff, approximately 925 ± 150 kg m^{-2} yr^{-1} of water are estimated to pass through the studied soil annually.

The soil water alkalinity in the deep soil was 2.59 ± 0.34 meq kg^{-1} based on the average of the measurements at 260 cm depth. The average alkalinity for the surface waters after oxidation and the precipitation of ferrihydrite calculated with PHREEQC is 1.53 ± 0.2 meq kg^{-1}. Multiplying this value by the estimated annual water flux through the soil yields an annual alkalinity export via surface waters of 1.45 ± 0.3 eq m^{-2} yr^{-1}. Multiplying this number by the atomic weight of carbon yields an annual carbon flux of 17 ± 3.6 g m^{-2} yr^{-1} or 0.17 ± 3.6 t ha^{-1} yr^{-1} of C. Note the long-term fate of this captured carbon may evolve once the river water transporting this carbon arrives in the oceans.

To extrapolate the annual mass of carbon drawdown to the gigaton scale, we divided one gigaton of CO_2, which is equal to $2.73x10^8$ tons of C by the 0.17 t ha^{-1} yr^{-1} of C drawdown in rivers provoked by the addition of basaltic dust to our field site. This yielded a surface area of $1.6x10^9$ ha. This surface area is

equal to $1.6x10^7$ km^2. This is larger than the surface area of the United States, which is equal to $9.8x10^6$ km^2. The mass of dust needed to be added to $1.6x10^7$ km^2 annually to attain the same 500–800 g m^{-2} yr^{-1} of dust added to our study site is obtained by multiplying this flux and surface area. This calculation yields 8 to $13x10^9$ t yr^{-1}, which equals 8 to 13 Gt yr^{-1}.

Estimated organic carbon storage within the studied soil

The mass of organic carbon in our studied soil was estimated by considering it is comprised of two parts, an upper part formed after the settlement (1076 year BP) and a lower part formed from 1076 down to 3,300 year BP (Fig. 1). This separation is based on the report of an increase in dust flux after this time [55]. These parts are divided based on the position of tephra layers that allow the direct determination of the net rates of soil accumulation, including the effects of soil erosion, over time. The upper part is a Gleyic Andosol containing < 12% C by dry weight extending down to ~ 90 cm, while the lower part is a Histic Andosol containing 12–20% C by dry weight from ~ 90 to 22 cm. These maximum soil carbon values of 12 and 20% were multiplied by the height of each soil section, assuming a porosity between 50 and 75% [39,40] to estimate the total carbon present in the studied soil. This calculation led to an estimated total mass of organic carbon equal to 86 to 172 kgC m^{-2} for a 75% and 50% soil porosity respectively. Further details of this calculation are provided in Table SI4. Dividing this mass by the 3,300-year age of the soil column yields an average organic carbon production rate of 26–52 gC m^{-2} yr^{-1}. Note that the mass of carbon in organic material, reported in units of mass of C can be converted to the equivalent mass CO_2 by multiplying the former by the ratios of their respective molar masses: 44/12.

Declarations

Acknowledgement:

The authors thank Knud Dideriksen for his comments and discussions during the field work. We thank the Icelandic meteorological office (Veðurstofa Íslands) for providing rainwater data, Liane Benning and her team at the Geological research centre GFZ Potsdam for the DOC measurements, Þorsteinn Jónsson for assisting in the field and designing coring equipment and Egill Erlendsson and Guðrún Gísladóttir at University of Iceland for helping with site selection. We thank Bryndís Róbertsdóttir at the National Energy Authority Iceland for her help with identifying the tephra layers and Eirikur Benjaminsson for access to his property incl. We thank Susan Stipp and Dominique Tobler, the Metal-Aid coordinators, as well as the network members for their pleasant company during this study. This project was funded by the European Union's Horizon 2020 research and innovation programme under the Marie Skłodowska-Curie grant agreement No 675219, from Landsvirkjun under the project number 2456, and the Icelandic Center for Research (Rannís) on behalf of the Doctoral Student Fund of the Ministry for the Environment and Natural Resources under the grant No 218929-051. Additional financial support was received from the

Research Fund of the University of Iceland and the Travel grant for doctoral students at the University of Iceland.

Author contribution:

T. Linke conducted the associated field and lab work, sample analysis and modelling. The field observations were interpreted and the manuscript was written by E.H. Oelkers and T. Linke in collaboration with S.R. Gislason and S.C. Moeckel. S.C. Moeckel described the soil profile and identified the soil layers. S.R. Gislason acquired the funding and helped with fieldwork.

Competing interests

All of the authors declare that there are no competing interests.

Data availably

The authors declare that all data supporting the findings of this study are available within the paper and its Supplementary Information. Cited data is available in the corresponding published references.

References

1. Gislason, S. R. & Eugster, H. P. Meteoric water-basalt interactions. II: A field study in N.E. Iceland. *Geochim. Cosmochim. Acta.* **51**, 2841-2855 (1987).
2. Gislason, S. R. *et al.* Direct evidence of the feedback between climate and weathering. *Earth Planet. Sci. Lett.* **277**, 213–222 (2009).
3. Dessert, C., Dupré, B., Gaillardet, J., François, L. M. & Allègre, C. J. Basalt weathering laws and the impact of basalt weathering on the global carbon cycle. *Chem. Geol.* **202**, 257–273 (2003).
4. Taylor, L. L. *et al.* Increased carbon capture by a silicate-treated forested watershed affected by acid deposition. *Biogeosciences* **18**, 169–188 (2021).
5. Moosdorf, N., Renforth, P. & Hartmann, J. Carbon dioxide efficiency of terrestrial enhanced weathering. *Environ. Sci. Technol.* **48**, 4809–4816 (2014).
6. IPCC. *Global warming of 1.5℃* An *IPCC Special Report on the impacts of global warming of 1.5℃* above *pre-industrial levels and related global greenhouse gas emission pathways, in the context of strengthening the global response to the threat of climate change, sustainable development, and efforts to eradicate poverty*. https://www.ipcc.ch/site/assets/uploads/sites/2/2019/06/SR15_Full_Report_High_Res.pdf (2018).
7. Beerling, D. J. *et al.* Potential for large-scale CO_2 removal via enhanced rock weathering with croplands. *Nature* **583**, 242–248 (2020).
8. Strefler, J., Amann, T., Bauer, N., Kriegler, E. & Hartmann, J. Potential and costs of carbon dioxide removal by enhanced weathering of rocks. *Environ. Res. Lett.* **13**, (2018).

9. Haque, F., Santos, R. M., Dutta, A., Thimmanagari, M. & Chiang, Y. W. Co-Benefits of Wollastonite Weathering in Agriculture: CO_2 Sequestration and Promoted Plant Growth. *ACS Omega* **4**, 1425–1433 (2019).
10. Haque, F., Santos, R. M. & Chiang, Y. W. CO_2 sequestration by wollastonite-amended agricultural soils – An Ontario field study. *Int. J. Greenh. Gas* **97**, (2020).
11. Amann, T. *et al.* Constraints on Enhanced Weathering and related carbon sequestration-a cropland mesocosm approach. *Biogeosci. Discuss.* 1–21 (2018).
12. Cho, Y., Driscoll, C. T., Johnson, C. E. & Siccama, T. G. Chemical changes in soil and soil solution after calcium silicate addition to a northern hardwood forest. *Biogeochemistry* **100**, 3–20 (2010).
13. Gillman, G. P., Burkett, D. C. & Coventry, R. J. Amending highly weathered soils with finely ground basalt rock. *Appl Geochem.* **17**, 987–1001 (2002).
14. ten Berge, H. F. M. *et al.* Olivine weathering in soil, and its effects on growth and nutrient uptake in ryegrass (Lolium perenne L.): A pot experiment. *PLoS One* **7**, (2012).
15. Haque, F., Chiang, Y. & Santos, R. Alkaline Mineral Soil Amendment: A Climate Change 'Stabilization Wedge'? *Energies* **12**, 2299 (2019).
16. Mahowald, N. M. *et al.* Atmospheric global dust cycle and iron inputs to the ocean. *Global Biogeochem. Cycles* **19**, (2005).
17. Arnalds, O. Dust sources and deposition of aeolian materials in Iceland. *Icel. Agric. Sci.* **23**, 3–21 (2010).
18. Arnalds, O., Dagsson-Waldhauserova, P. & Olafsson, H. The Icelandic volcanic aeolian environment: Processes and impacts - A review. *Aeolian Res.* **20**, 176–195 (2016).
19. Arnalds, O., Olafsson, H. & Dagsson-Waldhauserova, P. Quantification of iron-rich volcanogenic dust emissions and deposition over the ocean from Icelandic dust sources. *Biogeosciences* **11**, 6623–6632 (2014).
20. Liu, E. J. *et al.* Ash mists and brown snow: Remobilization of volcanic ash from recent Icelandic eruptions. J. Geophys. Res. Atmos. **119**, 9463–9480 (2014).
21. Baldo, C. *et al.* Distinct chemical and mineralogical composition of Icelandic dust compared to northern African and Asian dust. *Atmos. Chem. Phys.* **20**, 13521–13539 (2020).
22. Arnalds, O. *The Soils of Iceland*. *Springer* (2015). doi:10.1097/00010694-196104000-00017.
23. Arnalds, O. Volcanic soils of Iceland. *Catena* **56**, 3–20 (2004).
24. Shoji, S., Nanzyo, M. & Dahlgren, R. *Volcanic ash soils - Genesis, Properties and Utilization*. Developments in Soil Science **65** (1995).
25. Arnalds, O., Gudmundsson, J., Oskarsson, H., Brink, S. H. & Gisladottir, F. O. Icelandic Inland Wetlands: Characteristics and Extent of Draining. *Wetlands* **36**, 759–769 (2016).
26. Möckel, S. C., Erlendsson, E. & Gísladóttir, G. Holocene environmental change and development of the nutrient budget of histosols in North Iceland. *Plant Soil* **418**, 437–457 (2017).

27. Gísladóttir, G., Erlendsson, E., Lal, R. & Bigham, J. Erosional effects on terrestrial resources over the last millennium in Reykjanes, southwest Iceland. *Quat. Res.* **73**, 20–32 (2010).
28. Arnalds, Ó. Soils of Iceland. *Jökull* **58**, 409–421 (2008).
29. Xu, J., Morris, P. J., Liu, J. & Holden, J. PEATMAP: Refining estimates of global peatland distribution based on a meta-analysis. *Catena* **160**, 134–140 (2018).
30. Mitra, S., Wassmann, R. & Vlek, P. L. G. An appraisal of global wetland area and its organic carbon stock. *Curr. Sci.* **88**, 25–35 (2005).
31. Limpens, J. *et al.* Peatlands and the carbon cycle: From local processes to global implications - A synthesis. *Biogeosciences* **5**, 1475–1491 (2008).
32. Bragazza, L., Parisod, J., Buttler, A. & Bardgett, R. D. Biogeochemical plant-soil microbe feedback in response to climate warming in peatlands. *Nat. Clim. Chang.* **3**, 273–277 (2013).
33. Hooijer, A., Silvius, M., Wösten, H. & Page, S. PEAT-CO2, Assessment of CO2 emissions from drained peatlands in SE Asia. *Delft Hydraulic Report Q3943* (2006) 36 (2006).
34. Crump, J. *Smoke on water: countering global threats from peatlands loss and degradation. A UNEP rapid response assessment*. (UNEP Grid Arendal, 2017).
35. Parish, F. *et al.* Assessment on Peatlands, Biodiversity and Climate Change: Main Report. *Glob. Environ. Centre, Kuala Lumpur Wetlands International* 1–177 (2008).
36. Keller N. et al. *National Inventory Report - Emissions of greenhouse gases in Iceland from 1990 to 2018*. (The Environment Agency of Iceland, 2020).
37. Arnalds, O. & Óskarsson, H. Íslenskt jarðvegskort Íslenskur (A soil map of Iceland). *Náttúrufræðingurinn* **78**, 107–121 (2009).
38. Parkhurst, D. L. & Appelo, C. A. J. *USER'S GUIDE TO PHREEQC (VERSION 2)— A COMPUTER PROGRAM FOR SPECIATION, BATCH-REACTION, ONE-DIMENSIONAL TRANSPORT, AND INVERSE GEOCHEMICAL CALCULATIONS*. *Water-Resources Investigations Report* (1999) doi:10.2307/3459821.
39. Renforth, P. & Henderson, G. Assessing ocean alkalinity for carbon sequestration. *Rev. Geophys.* **55**, 636–674 (2017).
40. Moras, C. A., Bach, L. T., Cyronak, T., Joannes-Boyau, R. & Schulz, K. G. Ocean alkalinity enhancement-avoiding runaway $CaCO_3$ precipitation during quick and hydrated lime dissolution. *Biogeosciences* **19**, 3537–3557 (2022).
41. Hartmann, J. *et al.* Stability of alkalinity in ocean alkalinity enhancement (OAE) approaches-consequences for durability of CO 2 storage. *Biogeosciences* **20**, 781–802 (2023).
42. He, J. & Tyka, M. D. Limits and CO 2 equilibration of near-coast alkalinity enhancement. *Biogeosciences* **20**, 27–43 (2023).
43. Snæbjörnsson, Á. *Um Vatnsleiðnimælingar í Jarðvegi á nokkrum stöðum í Borgarfirði*. (1982).
44. Orradottir, B., Archer, S. R., Arnalds, O., Wilding, L. P. & Thurow, T. L. Infiltration in Icelandic Andisols: The Role of Vegetation and Soil Frost. *Arct. Antarct. Alp. Res.* **40**, 412–421 (2008).

45. Óskarsson, H., Arnalds, Ó., Gudmundsson, J. & Gudbergsson, G. Organic carbon in Icelandic Andosols: Geographical variation and impact of erosion. in *Catena* **56** 225–238 (2004).
46. Vicca, S. *et al.* Is the climate change mitigation effect of enhanced silicate weathering governed by biological processes? *Glob. Chang. Biol.* **28**, 711–726 (2022).
47. Goll, D. S. *et al.* Potential CO2 removal from enhanced weathering by ecosystem responses to powdered rock. *Nat. Geosci.* **14**, 545–549 (2021).
48. Angst, G. *et al.* Soil organic carbon stocks in topsoil and subsoil controlled by parent material, carbon input in the rhizosphere, and microbial-derived compounds. *Soil Biol. Biochem.* **122**, 19–30 (2018).
49. da Silva, Y. J. A. B. *et al.* Weathering rates and carbon storage along a climosequence of soils developed from contrasting granites in northeast Brazil. *Geoderma* **284**, 1–12 (2016).
50. Möckel, S. C., Erlendsson, E. & Gísladóttir, G. Andic Soil Properties and Tephra Layers Hamper C Turnover in Icelandic Peatlands. *J. Geophys. Res. Biogeosciences* **126**, (2021).
51. Möckel, S. C., Erlendsson, E., Prater, I. & Gísladóttir, G. Tephra deposits and carbon dynamics in peatlands of a volcanic region: Lessons from the Hekla 4 eruption. *Land Degrad. Dev.* **32**, 654–669 (2021).
52. Araujo, M. A., Zinn, Y. L. & Lal, R. Soil parent material, texture and oxide contents have little effect on soil organic carbon retention in tropical highlands. *Geoderma* **300**, 1–10 (2017).
53. Wang, H. *et al.* No tillage increases soil organic carbon storage and decreases carbon dioxide emission in the crop residue-returned farming system. *J. Environ. Manage.* **261**, 110261 (2020).
54. Shakoor, A. *et al.* A global meta-analysis of greenhouse gases emission and crop yield under no-tillage as compared to conventional tillage. *Sci. Total Environ.* **750**, (2021).
55. Li, Z. *et al.* Responses of soil greenhouse gas emissions to no-tillage: A global meta-analysis. *Sustain. Prod. Consum.* **36**, 479–492 (2023).
56. Saemundsson, K. Outline of the geology of Iceland. *Jökull* **29**, 7–28 (1979).
57. McDougall, I., Kristjansson, L. & Saemundsson, K. Magnetostratigraphy and Geochronology of Northwest Iceland. *J. Geophys. Res.* **89**, 7029–7060 (1984).
58. Norðdahl, H., Ingólfsson, Ó., Pétursson, H. G. & Hallsdóttir, M. Late Weichselian and Holocene environmental history of Iceland. *Jökull* **58**, 343–364 (2008).
59. Dugmore, A. J., Gisladóttir, G., Simpson, I. A. & Newton, A. Conceptual Models of 1200 Years of Icelandic Soil Erosion Reconstructed Using Tephrochronology. *J. North Atl.* **2**, 1–18 (2009).
60. Rydin, H. & Jeglum, J. K. *The Biology of Peatlands*. (Oxford University Press, 2013). doi:10.1093/acprof:osobl/9780199602995.001.0001.
61. Petersen, G. N. & Berber, D. *Jarðvegshitamælingar á Íslandi. Staða núverandi kerfis og framtíðarsýn*. (2018).
62. Grönvold, K. *et al.* Ash layers from Iceland in the Greenland GRIP ice core correlated with oceanic and land sediments. *Earth Planet. Sci. Lett.* **135**, 149–155 (1995).

63. Gísladóttir, G., Erlendsson, E. & Lal, R. Soil evidence for historical human-induced land degradation in West Iceland. *Appl. Geochem.* **26**, 2009–2012 (2011).
64. Schoeneberger, P. J., Wysocki, D. A., Benham, E. C. & Stuff, S. S. *Field Book for Describing and Sampling Soils*. (2012).
65. Sigfusson, B., Paton, G. I. & Gislason, S. R. The impact of sampling techniques on soil pore water carbon measurements of an Icelandic Histic Andosol. *Sci. Total Environ.* **369**, 203–219 (2006).
66. Sawyer, D. T., Roberts, J. L. & Sobkowiak, A. *Electrochemistry for chemists*. (Wiley, 1995).
67. Arnórsson, S. *Isotopic and Chemical Techniques in Geothermal Exploration, Development and Use*. (International Atomic Energy Agency, 2000).
68. Gran, G. Determination of the equivalence point in potentiometric Titrations. Part II. *Analyst* **77**, 661–671 (1952).
69. Kaasalainen, H., Stefánsson, A. & Druschel, G. K. Determination of Fe(II), Fe(III) and Fetotal in thermal water by ion chromatography spectrophotometry (IC-Vis). *Int. J. Environ. Anal. Chem.* **96**, 1074–1090 (2016).
70. Huber, S. A., Balz, A., Abert, M. & Pronk, W. Characterisation of aquatic humic and non-humic matter with size-exclusion chromatography - organic carbon detection - organic nitrogen detection (LC-OCD-OND). *Water Res.* **45**, 879–885 (2011).
71. Allison, J. D., Brown, D. S. & Novo-Gradac, K. J. *MINTEQA2/PRODEFA2—A geochemical assessment model for environmental systems—Version 3.0 user's manual*. (1991).
72. U.S. Environmental Protection Agency. *MINTEQA2/PRODEFA2, A Geochemical Assessment Model for Environmental Systems: User Manual Supplement for Version 4.0*. vol. 1998 (1998).
73. Jóhannesson, T. *et al.* Effect of climate change on hydrology and hydro-resources in Iceland. *Nat*iona*l Energy* Authority - Hydrological Service **OS-2007/011**, 91 (2007).
74. Sigurðsson, B. D., Bjarnadottir, B., Strachan, I. & Palmason, F. Tilraunaskógurinn í Gunnarsholti II - Vatnið í skóginum. *Skógræktarritið* **1**, 55–64 (2004).
75. Vitt, D. H., Bayley, S. E. & Jin, T.-L. Seasonal variation in water chemistry over a bog-rich fen gradient in Continental Western Canada. *Can. J. Fish. Aquat. Sci.* **52**, 587–606 (1995).
76. Dawson, J. J. C., Billett, M. F., Neal, C. & Hill, S. A comparison of particulate, dissolved and gaseous carbon in two contrasting upland streams in the UK. *J. Hydrol.* **257**, 226–246 (2002).
77. Bragazza, L., Rydin, H. & Gerdol, R. Multiple gradients in mire vegetation: A comparison of a Swedish and an Italian bog. *Plant Ecol.* **177**, 223–236 (2005).
78. Kulzer, L., Luchessa, S., Cooke, S., Errington, R. & Weinmann, F. Characteristics of the Low-Elevation Sphagnum-Dominated Peatlands of Western Washington: A Community Profile Part1: Physical, Chemical and Vegetation Characteristics. *King County, Washingt*on (2001).
79. Verry, E. *Streamflow Chemistry and Nutrient Yields from Upland-Peatland Watersheds in Minnesota*. *Ecology* **56,** 1149-1157 (1975).

Figures

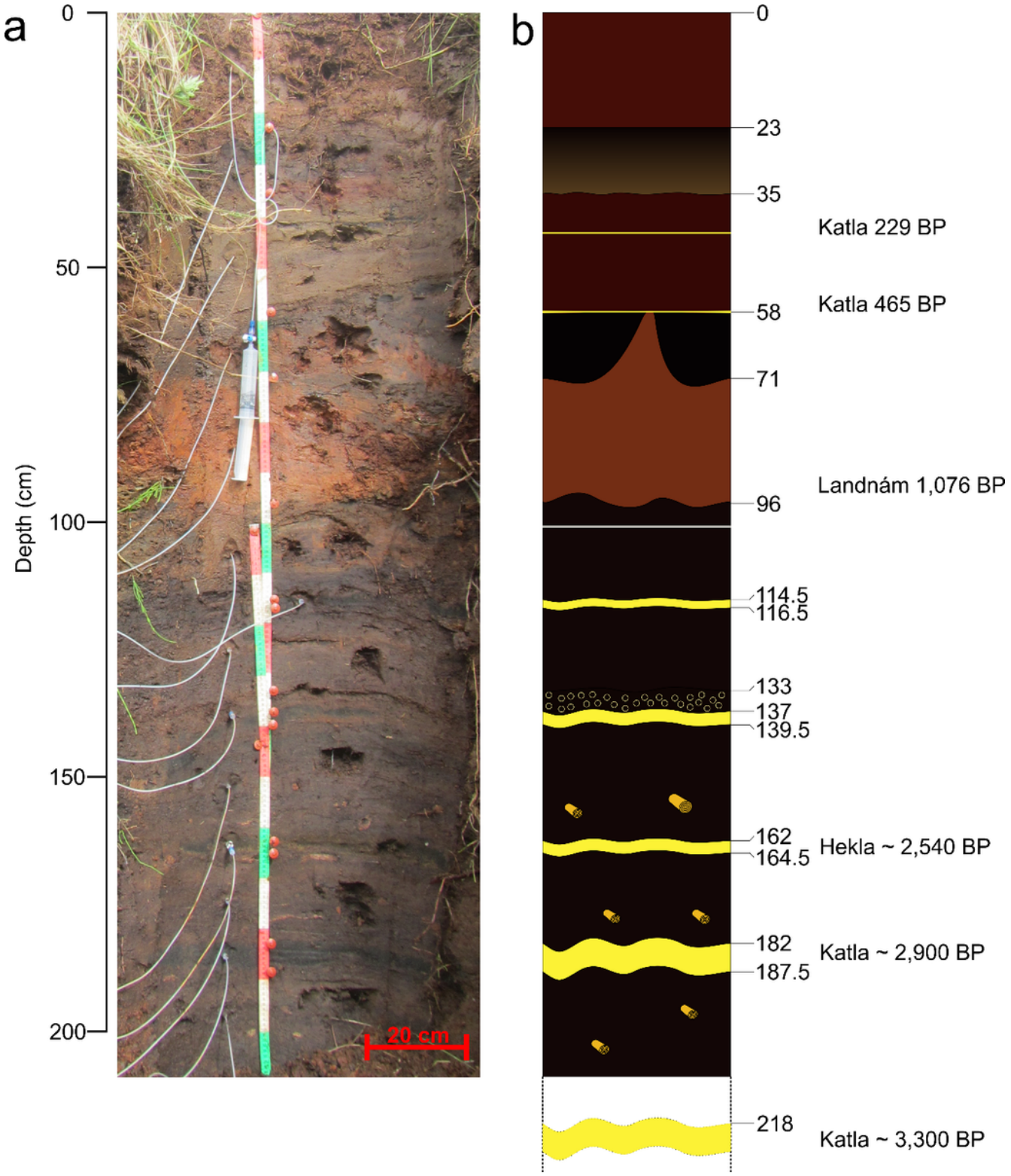

Figure 1

Outcrop of the studied soil section.

a, Photograph of the studied soil system. The dark layers correspond to tephra originating from historic volcanic eruptions. **b**, Schematic illustration of the soil profile with depths and ages (in years before present) of identified tephra layers shown in yellow for better visibility, the Landnám Layer that occurred around the time of the Icelandic settlement could not be clearly identified because of heavy alteration. Large plant remnants are visible in the lower part of the profile indicating high organic content.

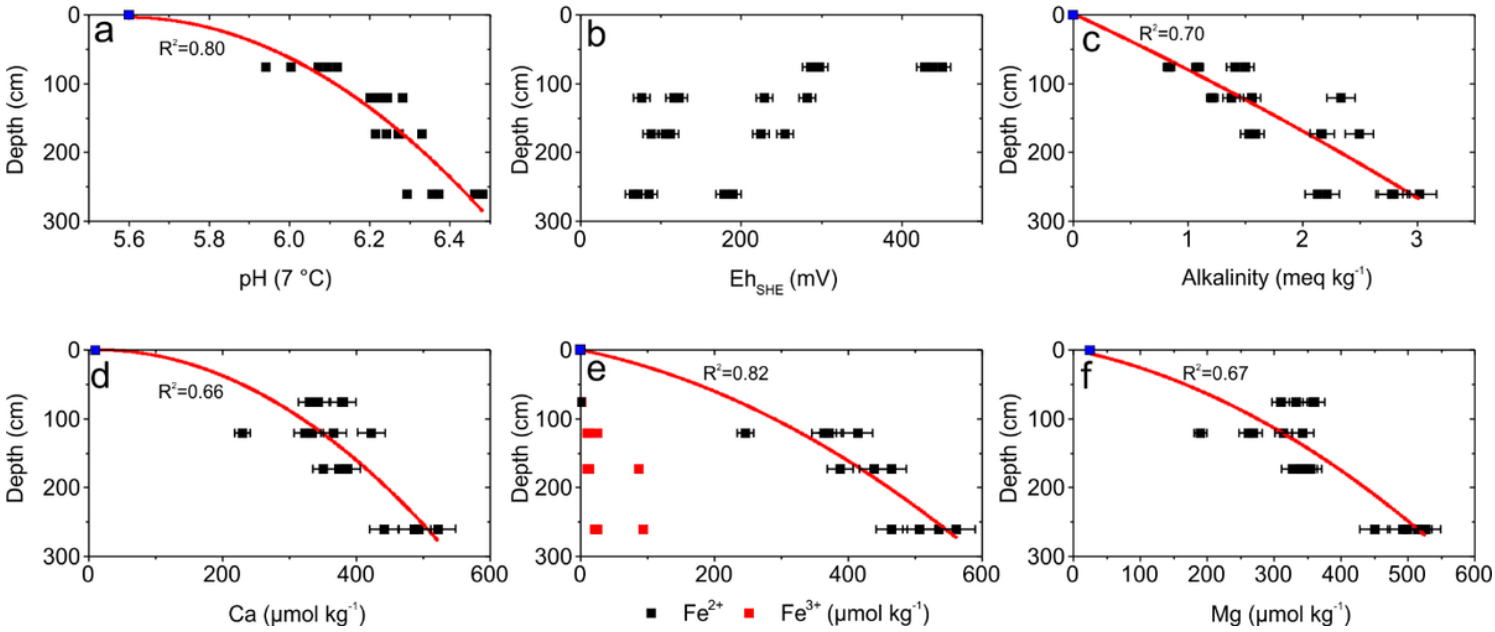

Figure 2

Measured soil water concentrations and best fit of the data.

a-f. Measured soil water concentrations determined in the present study versus depth. The pH values are normalized to a 7 °C reference temperature and Eh values to a Standard Hydrogen Electrode. The black squares represent measured water compositions whereas the blue square shows the composition of the rainwater. The error bars correspond to a ±5 % uncertainty on the measured concentrations; error bars do not appear if the uncertainty is smaller than the symbol size. The red curves in the figure show 2nd order polynomial fits of the measured concentrations with the corresponding R^2 values next to each curve.

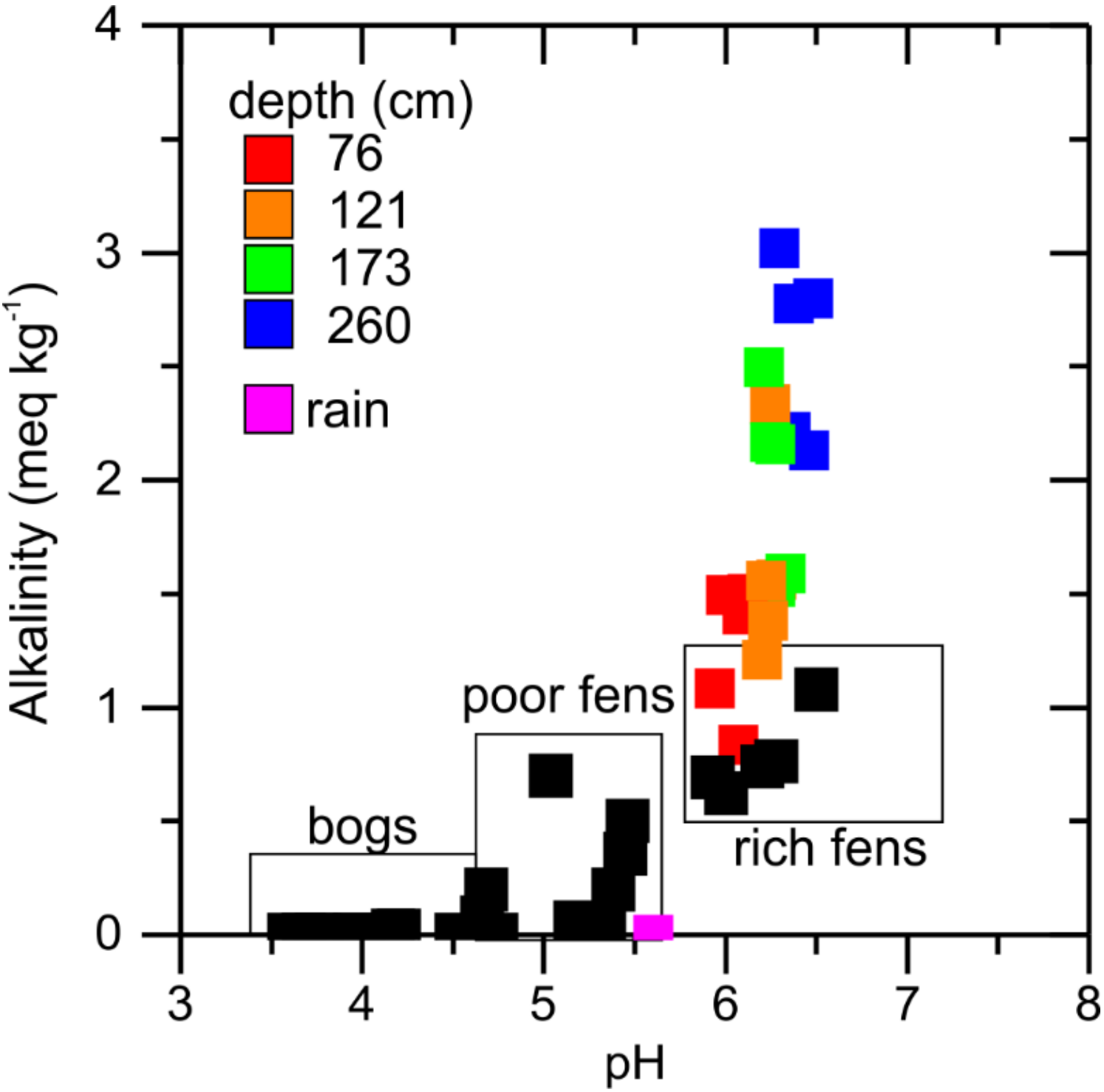

Figure 3

Comparison of pH and alkalinity of soil waters collected from the Histic/Gleyic Andosol soil in the present study with similarly composed, but volcanic dust-free Histosols reported in other studies.

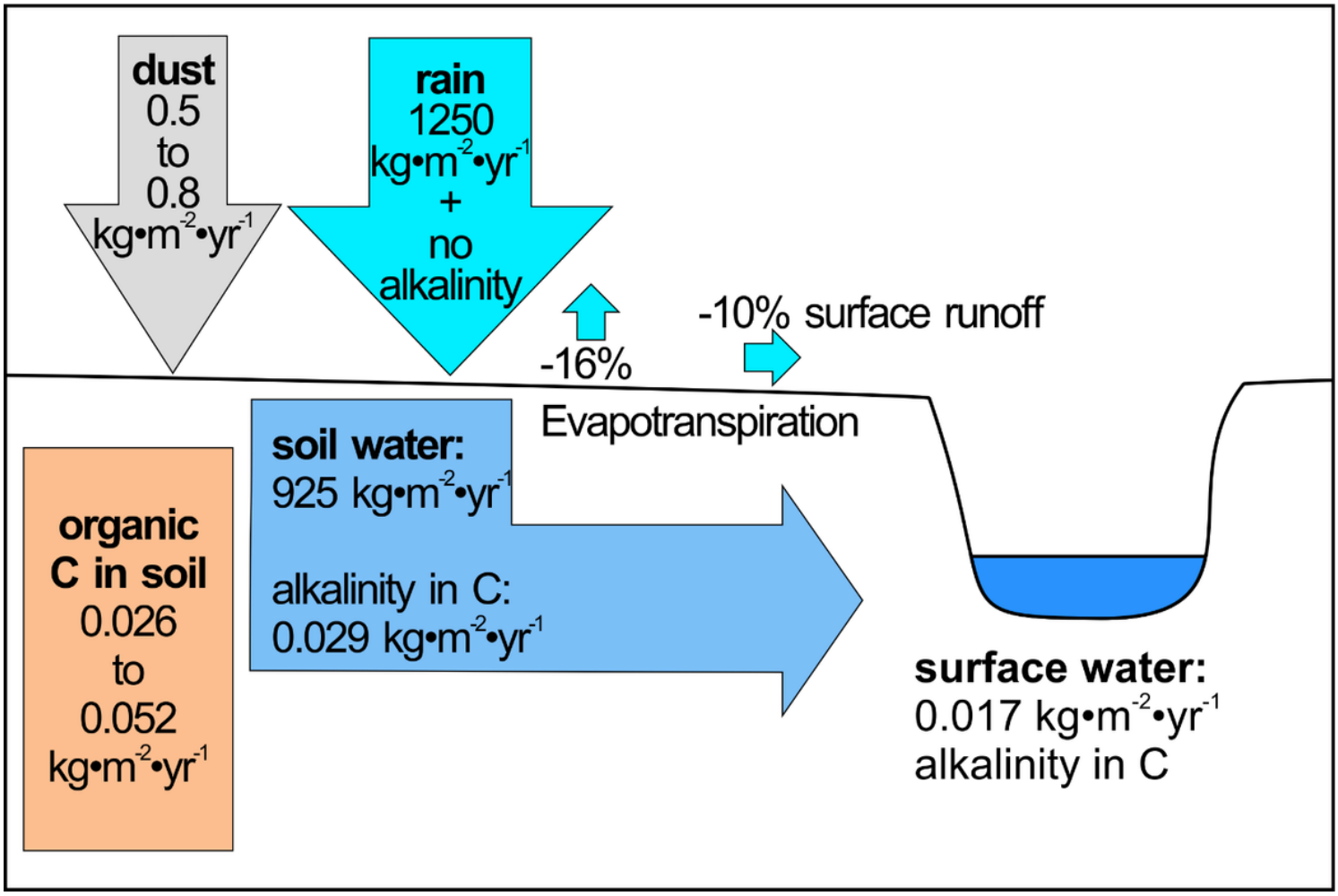

Figure 4

Fate of rainwater as it passes through our field site.

Supplementary Files

This is a list of supplementary files associated with this preprint. Click to download.

- SupplementaryInformation.docx